Wintertime Surface Winds over the Greenland Ice Sheet*

DAVID H. BROMWICH,[†] YANG DU,[†] AND KEITH M. HINES

Polar Meteorology Group, Byrd Polar Research Center, The Ohio State University, Columbus, Ohio

(Manuscript received 14 August 1995, in final form 25 March 1996)

ABSTRACT

Clear-sky, wintertime surface winds over the Greenland Ice Sheet are simulated with a three-dimensional mesoscale numerical model. It is shown that the simulated winds blow from the broad gently sloped interior to the steep coastal margins. This general wind pattern is similar to that found over Antarctica due to the same governing dynamics. The longwave radiational cooling of the sloping ice terrain is the key driving force of this cold airflow. In some coastal areas the downslope winds converge into large fjords, such as Kangerlussuaq and Sermilik. This is consistent with the frequent presence in these areas of warm signatures on cloud-free thermal infrared satellite images that are generated by katabatic winds. The shape of the Greenland Ice Sheet plays an important role in directing the flow of the surface winds. The study demonstrates that the surface wind pattern is only moderately affected by climatological flow around and over the ice sheet. The mass redistribution associated with the katabatic wind circulation plays an important role in generating prominent features of the time-averaged sea level pressure and upper-level circulation fields near Greenland.

1. Introduction

Greenland, about the same size as the Tibetan Plateau, is the largest ice-capped terrain in the Northern Hemisphere and one of the least studied areas from a meteorological perspective. Because the radiative characteristics and boundary layer dynamics resemble those of Antarctica, which is located in the Southern Hemisphere (Schwerdtfeger 1972), similar surface wind features were observed by early expeditions (Manley 1938) and are found on modern satellite imagery (Rasmussen 1989; Bromwich 1989). The latter often shows winter katabatic (downslope) winds over the ice sheet when skies are clear.

Figure 1 shows a two-dimensional view of the topography of Greenland used in this study, with geographic features labelled. The terrain features are somewhat simpler than those of Antarctica. Overall, slopes from the interior to the east coast are steeper than those to the west coast. Prominent fjords, such as Kangerlussuaq and Sermilik, are located in the southeast coastal margins. It can be inferred that the surface wind field features over the Greenland Ice Sheet should to some extent be similar to those over Antarctica because the governing dynamics are similar. The composite wind patterns over the ice sheet were qualitatively analyzed from the thermal field detailed by satellite images (Rasmussen 1989). This analysis shows that the wind direction deviates to the right from the downslope direction due to the Coriolis effect. The most significant convergence is found around Kangerlussuaq Fjord. This kind of wind pattern can result in a dark signature on thermal infrared satellite images (Rasmussen 1989), propagating from the ice sheet for more than 100 km over Denmark Strait. The dark signature arises because of warming of the ice surface by vertical mixing associated with turbulent katabatic winds. Data obtained at weather stations demonstrate that over the gently sloping central part of Greenland, the wind is light or moderate. The air blows in a more downslope direction as it moves away from the crest of the ice sheet. The wind accelerates with the increasing slope toward to the coastal margins. Well-developed summer katabatic winds were observed at a southwestern station during the Greenland Ice Margin Experiment (Oerlemans and Vugts 1993). The behavior of the katabatic winds over the edge of the Greenland Ice Sheet is important to the energy balance of the melting ice in the ablation zone during summer (Meesters 1994).

2. Methodology

In this paper, numerical simulations of wintertime (no solar radiation) surface winds over the Greenland Ice Sheet under clear sky conditions are conducted using a three-dimensional, hydrostatic, primitive equation model. Longwave radiation, which drives the cooling

* Contribution Number 1006 of Byrd Polar Research Center.

[†] Also affiliated with Atmospheric Sciences Program, The Ohio State University.

Corresponding author address: Prof. David H. Bromwich, Polar Meteorology Group, Byrd Polar Research Center, The Ohio State University, 108 Scott Hall, Columbus OH 43210-1002.

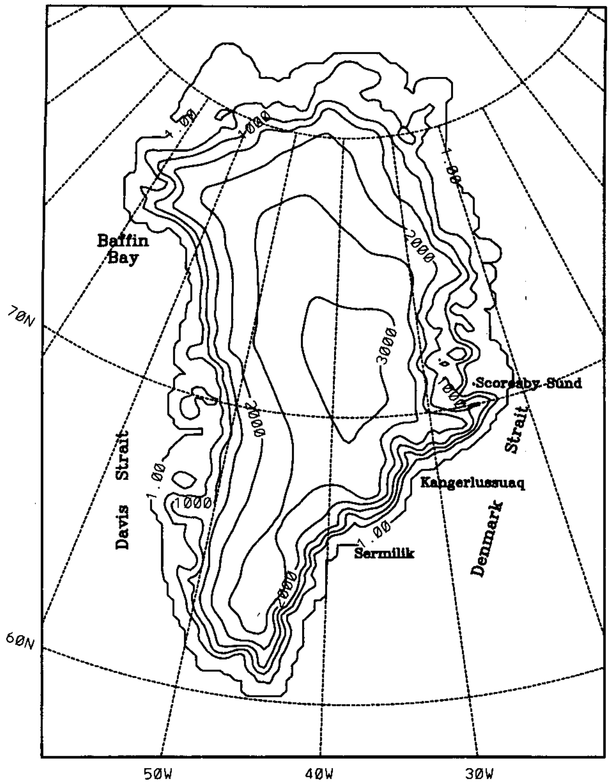

FIG. 1. Greenland Ice Sheet terrain used in the model. The contour interval is 500 m. The outermost contour represents the coastline.

at the surface within the katabatic layer, is treated with Cerni and Parish's (1984) cloud-free scheme. Within the boundary layer, turbulent fluxes, which frequently carry large quantities of heat from the katabatic layer to the surface, are obtained following Businger et al. (1971) and Brost and Wyngaard (1978). Indicative of the success of these key parameterizations, the model has been shown to be capable of realistically simulating the surface winds over Antarctica (Parish and Waight 1987; Parish 1992; Bromwich et al. 1994). The model domain consists of 100 × 150 horizontal grid points and 10 sigma levels (0.996, 0.985, 0.97, 0.95, 0.93, 0.90, 0.80, 0.60, 0.35, 0.10) in the vertical.

The Greenland topography, as shown in Fig. 1, is taken from a digitized map that provides an up-to-date depiction of the ice terrain (S. Ekholm 1995, personal communication). Airborne echo sounding observations from northern Greenland and ground-based global positioning system (GPS) elevations from the ice sheet summit are included. The height data are interpolated from the digitized map with a grid spacing of 0.02° in latitude by 0.06° in longitude to the model's horizontal grid with a resolution of 20 km.

For the initial conditions, a horizontally uniform temperature profile is taken from climatological charts (Crutcher and Meserve 1970). Two runs are examined. One (run 1) starts from a state of rest, and the other (run 2) starts from a prescribed pressure gradient taken from average winter pressure fields (Crutcher and Meserve 1970). The ocean surrounding Greenland is taken to be ice-free and at constant surface temperature in the simulations presented here. Experiments performed with a solid ice cover show little effect of peripheral ocean conditions on winds over Greenland. Here we report the results from the simulations with the case of open-water conditions beyond the margin of the ice sheet. The general pattern of the surface winds over Greenland is emphasized.

Both run 1 and run 2 are integrated for 24 h, by which time the surface winds have reached approximately steady-state conditions. Parish (1992) has extensively studied the time behavior of this model with idealized simulations of Antarctic winds. Much longer integrations would exhibit significant slowing of the surface winds due to the adverse pressure gradient associated with the strengthening upper-level cyclonic circulation (Parish 1992; Egger 1985), but this situation is disrupted by transient cyclones (Juckes et al. 1994) that are not considered in this idealized framework.

3. Results

Figure 2a shows the simulated streamlines at the lowest level (about 20 m above the surface) from run 1 after 24-h integration. The winds blow downward and to the right of the downslope direction due to the Coriolis effect. The dominant influence of Greenland topography on the surface airflow is seen. The flow pattern is quite uniform in the interior. Some coastal areas of confluence are evident, most prominently near Sermilik and Kangerlussuaq. This is consistent with the satellite observations (Rasmussen 1989). Divergence around the terrain ridge between Sermilik and Kangerlussuaq is shown, which is also evident on thermal infrared satellite images (see Fig. 2 in Rasmussen 1989). Unlike the winds along the Antarctic periphery (Parish and Bromwich 1991), the Greenland coastal wind pattern is more uniform. In general, the wind pattern is reminiscent of that over Antarctica for which the mechanisms of formation and maintenance of the katabatic winds have been studied extensively (Schwerdtfeger 1984). The strong cooling of the air adjacent to the sloping ice sheet results in a horizontal pressure gradient directed downslope. The forcing is proportional to the slope of the ice terrain (Ball 1960).

The simulated wind speeds at the lowest level are presented in Fig. 2b. Wind speeds around 12 m s^{-1} are present near the Greenland coastline. The maximum value of 16 m s^{-1} is located in northeastern Greenland. Wind speeds less than 3 m s^{-1} are located over the interior around the crest of the ice sheet. This speed pattern is consistent with the spatial distribution of terrain slopes.

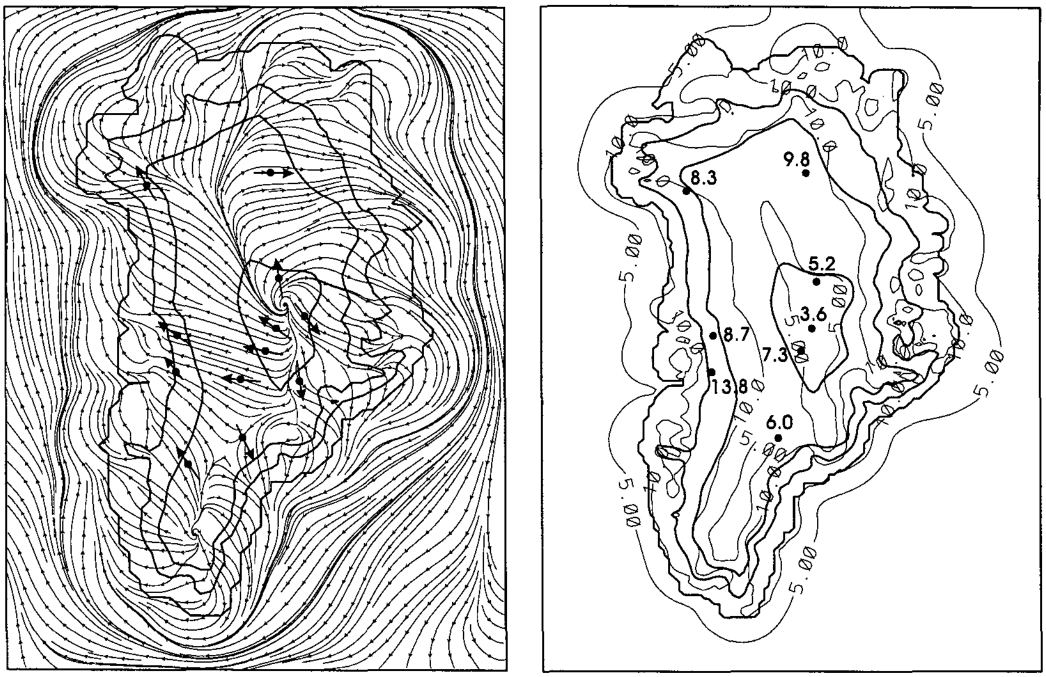

FIG. 2. (a) Streamlines at the lowest sigma level for the run with quiescent initial conditions (run 1). Arrows display observed wind directions from Table 1. The terrain contour (bold) interval is 1000 m. (b) Wind speed at the lowest level from run 1. Contour interval is 5 m s^{-1}. Observed speeds from Table 1 are plotted at dots.

Meteorological data for the Greenland Ice Sheet are very limited. Only a handful of manned sites, unevenly scattered over the ice sheet, have observations, and these are usually short and/or discontinuous. Also, these observations are concentrated in the southern half of Greenland. For comparison with the simulated wind field, prevailing surface winds are analyzed from historic manned sites (Haywood and Holleyman 1961; Hogue 1964; Putnins 1970) and vector-average winds from several recently deployed automatic weather sta-

TABLE 1. Observed winter (DJF) winds on the ice sheet for a variety of time periods compared to the model results. For the first three automatic weather station sites resultant directions and speeds (m s^{-1}) are given; speeds have been adjusted to first model level at 20 m. For the manned sites, prevailing directions and mean speeds (when available and vertically extrapolated) are presented.

	Locality			Observed data		Run 1		Run 2	
	Latitude	Longitude	Elevation (m)	Speed (m s^{-1})	Direction	Speed (m s^{-1})	Direction	Speed (m s^{-1})	Direction
ETH/UC Camp[a]	69°34′N	49°17′W	1157	13.8	130°	13.7	115°	13.8	109°
Barber[a]	71°40′N	38°10′W	3170	3.6	125°	2.7	105°	3.8	170°
Northice[b,d]	78°04′N	38°29′W	2342	9.8	270°	9.4	267°	8.5	270°
Camp Watkins[b,d]	67°03′N	41°49′W	2438	6.0	330°	5.4	345°	3.4	10°
Matt[a]	73°29′N	37°37′W	3100	5.2	170°	2.8	210°	4.0	200°
West Station[c,d]	71°11′N	51°07′W	954	8.7	113°	13.0	102°	13.6	111°
Central/Eismitte[c,d]	70°55′N	40°38′W	3025	7.3	98°	4.5	107°	5.3	123°
Hiran 30[d]	69°33′N	43°10′W	2545	—	90°	6.5	113°	6.4	120°
Century[d]	77°10′N	61°08′W	1923	8.3	128°	10.1	60°	10.7	60°
Hiran 27[d]	69°23′N	35°55′W	2758	—	354°	10.9	350°	11.0	340°
Julie[a]	72°34′N	34°38′W	3100	—	324°	4.9	323°	5.2	293°
Mint Julip[d]	66°16′N	47°46′W	1829	—	135°	9.9	135°	11.3	145°

[a] AWS.
[b] From Haywood and Holleyman (1961).
[c] From Putnins (1970).
[d] From Hogue (1964).

tions (AWS) whose data were obtained from the University of Wisconsin—Madison and from the University of Colorado at Boulder. The observations and the corresponding simulated winds from run 1 are listed in Table 1. The observed 3-m AWS speeds are extrapolated to the lowest model level with the assumption of a logarithmic profile in the vertical and $z_0 = 2 \times 10^{-4}$ m (compare Budd et al. 1966). The same vertical extrapolation is assumed to apply to the observed speeds from manned sites that were probably measured by near-surface instrumentation. Generally, the simulated wind directions show close similarity with the observations (Fig. 2a). The wind direction differences between the observed and simulated are within about 15° for many locations (Table 1). In particular, the differences at AWS Julie, and the manned sites of Northice, Hiran 27 and Mint Julip are within 5°. From Fig. 2a, these sites well represent the ice sheet topography. The largest difference (68°) occurs at Century, which is located on a gentle ridge. The model does not capture such small-scale topographic features.

ETH/University of Colorado Camp is located at the west coast of Greenland. The one winter (1993–1994) vector-average wind at this AWS is 13.8 m s^{-1} from 130°. The simulated wind speed and direction from the corresponding location is 13.7 m s^{-1} from 115°. The simulated wind speeds at AWS Barber and the manned sites of Northice and Camp Watkins are within several tenths of a meter per second of those observed. The simulated wind speed at AWS Matt is 2.8 m s^{-1}, which is lighter than the observed 5.2 m s^{-1}. Overall, the wind speeds are relatively well simulated (Fig. 2b), with greater success being obtained below 2500-m elevation because the terrain slopes are steeper. This is similar to the simulations over Antarctica (Parish and Bromwich 1991).

As discussed earlier, downslope winds over the Greenland Ice Sheet are due to strong cooling of the sloping terrain, which generates a strong horizontal pressure gradient directed in a downslope sense. Marked horizontal divergence occurs in the lowest layers of the atmosphere as a result of the predominant radial drainage off the elevated ice cap. Conservation of mass requires subsiding motion in the midtroposphere and hence upper-level convergence. This can be inferred from Fig. 3 in which simulated 500-hPa height for the first run after the 24-h integration is plotted for the entire model domain. The heights were calculated using an upward integration of the hydrostatic equation; temperatures were linearly interpolated between the sigma levels. It can be seen that a well-developed low is established over the crest of Greenland. The geostrophic wind circulations undergo a reversal with height, from anticyclonic to cyclonic, because of the horizontal temperature gradients.

It can be seen that the 500-hPa height field is markedly influenced by the Greenland topography. Because the terrain slopes on the eastern side are steeper than

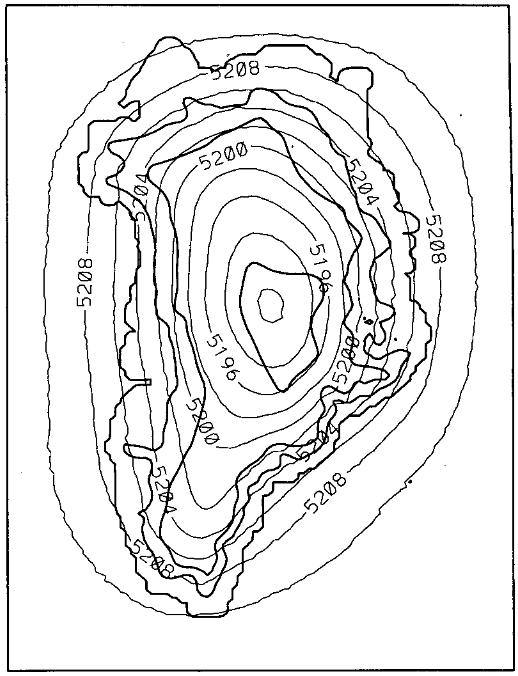

FIG. 3. The 500-hPa heights for the quiescent initial condition run after 24-h integration. Contour interval is 2 gpm.

those on the western side of Greenland, the gradient of the 500-hPa height contours is slightly sharper to the east than to the west. This is consistent with a simulation of the Antarctic katabatic wind circulation (Parish and Bromwich 1991). It is found that the geopotential height gradient over East Antarctica where the ice slopes are steepest is stronger than over West Antarctica where the terrain slopes are gentle. Comparing the simulated 500-hPa height field for Greenland with the one in Parish and Bromwich (1991) for Antarctica, an important point can be noted. The difference of height from the Greenland interior to the periphery is roughly 17 geopotential meters (gpm), while in the Antarctic simulation, a 60-gpm difference was obtained. This is a factor of 3.5 different. The area of Antarctica (14×10^6 km^2) is about a factor of 7 larger than that of Greenland (2×10^6 km^2). The ratio of the vortex strengths is about one-half that of the respective drainage areas. This occurs because the tropospheric vorticity buildup is forced by the cross-coastal mass transport associated with the drainage flow. This shows that the larger the drainage area, the stronger the overlying vortex.

Run 2 is initialized with the same pseudoanalytic technique used in Bromwich et al. (1994). The slightly baroclinic atmosphere is in hydrostatic and geostrophic balance. The initial sea level pressure field is a specified approximation to the climatological winter pressure field (Fig. 4a). A closed low is present in the southeastern section of the domain, while the gradient is very

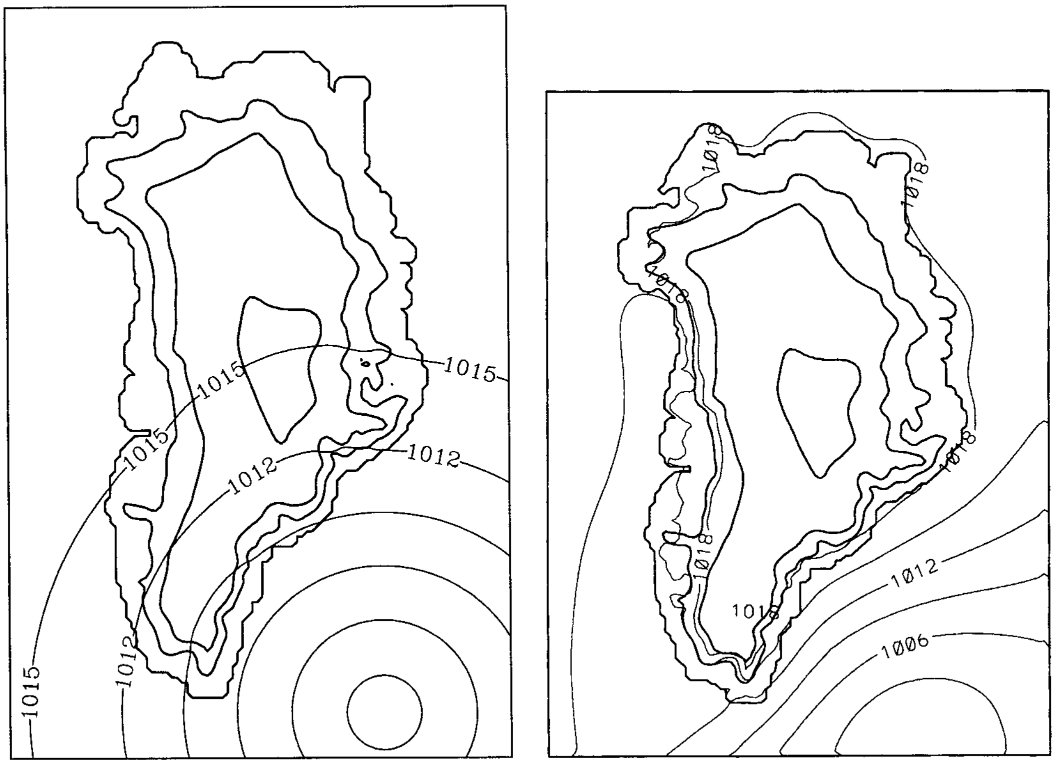

FIG. 4. Sea level pressure from run 2 (a) for initial field and (b) after 24-h integration. Contour interval is 3 hPa. Contours suppressed over elevated terrain in (b).

weak in the northern half. The streamlines at 24 h for the model's lowest level are shown in Fig. 5. The near-surface wind pattern over the Greenland ice terrain is nearly identical to that of run 1 (Fig. 2), but with 2 m s^{-1} or so stronger wind speeds in the coastal areas. Wind speeds from run 2 at nearly all locations are slightly stronger than those from run 1 (Table 1). Airflows around Kangerlussuaq fjord exhibit more pronounced confluence. Basically, the locations of the wind speed maxima remain unchanged. These results imply that the sloping terrain is the most important factor in shaping the downslope winds. The strong winds are driven mainly by radiative cooling of the sloping ice sheet.

Figure 4b illustrates the sea level pressure field after 24 h for run 2; substantial mass readjustment has taken place during the model integration, especially in the immediate vicinity of Greenland. The simulated low pressure trough to the west of the Greenland Ice Sheet (see Fig. 5 also) is a common feature on wintertime climatological maps (Crutcher and Meserve 1970). The blocking effect of the topography is evident. The pressure field results from the mass redistribution during the model integration. Figure 6a shows the idealized initial 500-hPa heights, with an upper-level high specified to the southeast of the Greenland Ice Sheet

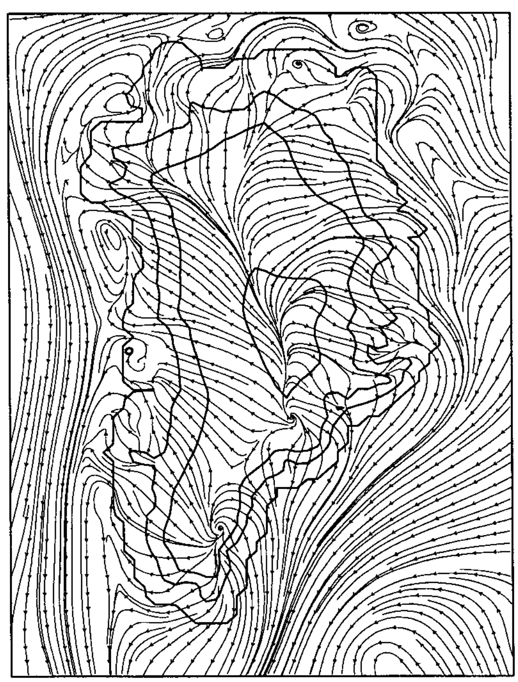

FIG. 5. The same as Fig. 2a but for run 2. The terrain contour interval is 1000 m.

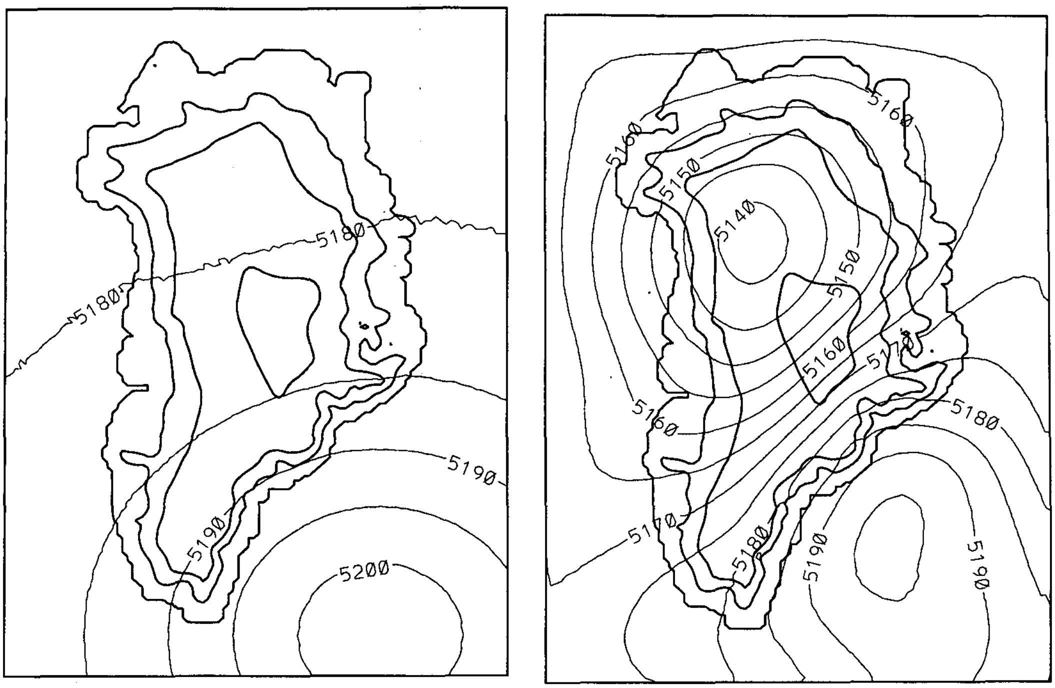

FIG. 6. The 500-hPa heights from run 2: (a) for initial field and (b) after 24-h integration. Contour interval is 5 gpm.

that approximates the observed ridge. Hydrostatically, this high overlies the low near the surface due to the heating from the relatively warm ocean. During the course of integration a cyclonic circulation becomes well established over the Greenland ice terrain (Fig. 6b) to the northwest of the anticyclonic circulation, which persists in a weakened and distorted state just offshore. The simulated low over Greenland probably contributes to the development of the climatological 500-hPa winter low that is situated just to the west-northwest of the ice sheet. This significant mass redistribution in Fig. 6 is associated with the Greenland katabatic wind circulation near the surface. The substantial impact of the katabatic winds on the upper-level atmospheric circulation is evident.

4. Conclusions

Numerical simulations of katabatic winds over the Greenland Ice Sheet during winter have been conducted. Compared with available observational data, the terrain-induced katabatic winds are reasonably well simulated. Strong and persistent katabatic winds downwind of confluence zones are sustained by cold airflow from the broad interior section. The Sermilik and Kangerlussuaq confluence zones are captured by the model. It is shown that the cross-coastal mass transport associated with the drainage flow is responsible for the tropospheric vorticity buildup over the ice sheet. The model results suggest that the surface wind pattern over the Greenland interior is only moderately affected by climatological flow over and beyond the ice-sheet margin. Simulations incorporating cloud effects and time-varying pressure gradients are needed to explore the impact of synoptic forcing on the surface winds over Greenland.

Acknowledgments. This research was supported by the Office of Polar Programs of the National Science Foundation via Grant OPP-9218949 to the first author. The digitized Greenland map used was kindly provided by Simon Ekholm, National Survey & Cadastre, Denmark. AWS data for Barber, Matt and Julie sites were obtained from Charles R. Stearns, University of Wisconsin—Madison, and for ETH/UC Camp from Konrad Steffen, University of Colorado at Boulder. The helpful comments of two anonymous reviewers are appreciated.

REFERENCES

Ball, F. K., 1960: Winds on the ice slopes of Antarctica. *Antarctic Meteorology, Proceedings of the Symposium in Melbourne, 1959,* Pergamon Press, 9–16.

Bromwich, D. H., 1989: Satellite analyses of Antarctic katabatic wind behavior. *Bull. Amer. Meteor. Soc.,* **70,** 738–749.

——, Y. Du, and T. R. Parish, 1994: Numerical simulation of winter katabatic winds from West Antarctica crossing Siple Coast and the Ross Ice Shelf. *Mon. Wea. Rev.,* **122,** 1417–1435.

Brost, R. A., and J. C. Wyngaard, 1978: A model study of the stably stratified planetary boundary layer. *J. Atmos. Sci.,* **35,** 1427–1440.

Budd, W. F., W. R. T. Dingle, and U. Radok, 1966: The Byrd snow drift project: Outline and basic results. *Studies in Antarctic Meteorology,* M. J. Rubin, Ed., Antarctic Research Series, Vol. 9, Amer. Geophys. Union., 71–134.

Businger, J. A., J. C. Wyngaard, Y. Izumi, and E. F. Bradley, 1971: Flux-profile relationships in the atmospheric surface layer. *J. Atmos. Sci.,* **28,** 181–189.

Cerni, T. A., and T. R. Parish, 1984: A radiative model of the stable nocturnal boundary layer with application to the polar night. *J. Climate Appl. Meteor.,* **23,** 1563–1572.

Crutcher, H. L., and J. M. Meserve, 1970: Selected level heights, temperatures, and dew points for the Northern Hemisphere. NAVAIR Rep. 50-1C-52, 426 pp. [Available from Superintendent of Documents, U.S. Government Printing Office, Washington, DC 20401.]

Egger, J., 1985: Slope winds and the axisymmetric circulation over Antarctica. *J. Atmos. Sci.,* **42,** 1859–1867.

Haywood, L. J., and J. B. Holleyman, 1961: Climatological means and extremes on the Greenland Ice Sheet. U.S. Army Corps Engrs., Cold Regions Res. Eng. Lab. Res. Rep. 78, 22 pp. [Available from U.S. Army CRREL, 72 Lyme Road, Hanover, NH 03755.]

Hogue, D. W., 1964: Environment of the Greenland ice cap. Tech. Rep. ES-14, 119 pp. [Available from World Data Center A for Glaciology, University of Colorado, Campus Box 449, Boulder, CO 80307.]

Juckes, M. N., I. N. James, and M. Blackburn, 1994: The influence of Antarctica on the momentum budget of the southern extratropics. *Quart. J. Roy. Meteor. Soc.,* **120,** 1017–1044.

Manley, G., 1938: Meteorological observations of the British East Greenland Expedition 1935–1936. *Quart. J. Roy. Meteor. Soc.,* **64,** 253–276.

Meesters, A., 1994: Dependence of the energy balance of the Greenland ice sheet on climate change: Influence of katabatic wind and tundra. *Quart. J. Roy. Meteor. Soc.,* **120,** 491–517.

Oerlemans, J., and H. F. Vugts, 1993: A meteorological experiment in the melting zone of the Greenland Ice Sheet. *Bull. Amer. Meteor. Soc.,* **74,** 355–365.

Parish, T. R., 1992: On the interaction between Antarctic katabatic winds and tropospheric motions in the high southern latitudes. *Aust. Meteor. Mag.,* **40,** 149–167.

——, and K. T. Waight, 1987: The forcing of Antarctic katabatic winds. *Mon. Wea. Rev.,* **115,** 2214–2226.

——, and D. H. Bromwich, 1991: Continental-scale simulation of the Antarctic katabatic wind regime. *J. Climate,* **4,** 135–146.

Putnins, P., 1970: The climate of Greenland. *Climates of the Polar Regions,* S. Orvig, Ed., Elsevier, 3–128.

Rasmussen, L., 1989: Greenland winds and satellite imagery. *VEJRET* (in English), N. W. Nilsen, Ed., Danish Meteorological Society, 32–37.

Schwerdtfeger, W., 1972: The vertical variation of the wind through the friction-layer over the Greenland ice cap. *Tellus,* **24,** 13–16.

——, 1984: *Weather and Climate of the Antarctic.* Elsevier Science, 261 pp.